J. Appl. Comput. Mech., 7(2) (2021) 890-901
DOI: 10.22055/JACM.2021.35741.2725

ISSN: 2383-4536
jacm.scu.ac.ir

Shahid Chamran University of Ahvaz

Journal of Applied and Computational Mechanics

Research Paper

Parameter Estimation in Population Balance through Bayesian Technique Markov Chain Monte Carlo

Carlos H.R. Moura[1], Bruno M. Viegas[2], Maria R.M. Tavares[2], Emanuel N. Macêdo[1,3], Diego C. Estumano[4], João N.N. Quaresma[1,3]

[1] Graduate Program in Chemical Engineering, PPGEQ/ITEC/UFPA, Federal University of Pará, 66075-110, Belém, PA, Brazil

[2] Graduate Program in Mathematics and Statistics, Federal University of Pará, Belém, PA, Brazil

[3] Graduate Program in Natural Resource Engineering in the Amazon, PRODERNA/ITEC/UFPA, Federal University of Pará, Belém, PA, Brazil

[4] Faculty of Biotechnology and Bioprocess Engineering, Federal University of Pará, Belém, PA, Brazil

Received November 14 2020; Revised December 29 2020; Accepted for publication January 04 2021.
Corresponding author: João N. N. Quaresma (quaresma@ufpa.br)

Abstract. In this work, the Markov Chain Monte Carlo is applied to estimate parameters that represent mechanisms that describe particles' dynamics in particulate systems from the literature's proposed models. Initially, the reduced sensitivity coefficient is evaluated to verify which parameters could be estimated simultaneously. The technique is then applied to estimate the models' parameters in different numerical scenarios to determine the rates that influence population dynamics. After the analyzes are performed, the estimates show good precision, accuracy, and a good fit between the measured and estimated state variables. The results show that the Markov chain Monte Carlo can determine the rates of population balance phenomenon.

Keywords: Particulate Systems, Population Balance, Bayesian Statistics, Markov Chain Monte Carlo.

1. Introduction

In the last decades, particulate processes have gained significant prominence in the engineering area, mainly for their crystallization applications, microbial cell culture bioreactors, emulsion, and suspension polymerization [1-3]. The most particulate processes' two significant properties are the size and particle size distribution, as these directly affect the desired final product. [4,5]. In these processes, determining the particle size distribution dynamics presupposes knowledge of the mechanisms of nucleation, growth, and aggregation of the particles. Quantitatively, this description is selected from the solution of the population balance equation (PBE) since this model simulates the dynamics of particulate processes [6,7].

The population balance equation describes several ways particles of a specific state can form or disappear from the system. The population balance represents the particle size distribution dynamics as they are created, broken, grown, entered, or left the control volume. Since the population balance equation simulates the change over time of the number of particles in a size range within the population process conditions, it is necessary to know the phenomena that can modify the distribution of particles over time, these being nucleation, growth, breakage, and aggregation [7,8].

In this field research, considerable difficulty is determinate the parameters from the mathematical models. Therefore, it is necessary to apply statistical techniques to estimate such parameters and describe the physical process through the inference of parameters.

These phenomena are represented within the population balance structure through rates that have parameters that can be estimated. The estimation of parameters within the population balance area has been researched in recent years [9-12]. Since obtaining these parameters is essential for understanding the mechanisms that control the distribution of particles and how they interact with the process variables, it is necessary to estimate these parameters to understand these mechanisms' rates. Usually is used classical statistic (Least-square), optimization techniques (bees algorithm, particle swarm) considering as cost function the norm of residual [13,14]. Although the literature shows some techniques to estimate parameters in the population balance model, the Bayesian methods were not applied yet in such physical phenomena. In this way, this work has the primary goal of showing Markov Chain's application to estimate the population balance model parameters. Recently, Markov Chain Monte Carlo has been applied in such fields as double spinel compounds [15], stochastic block model [16] and prompt gamma ray (PG) imaging [17].

Published online: January 07 2021

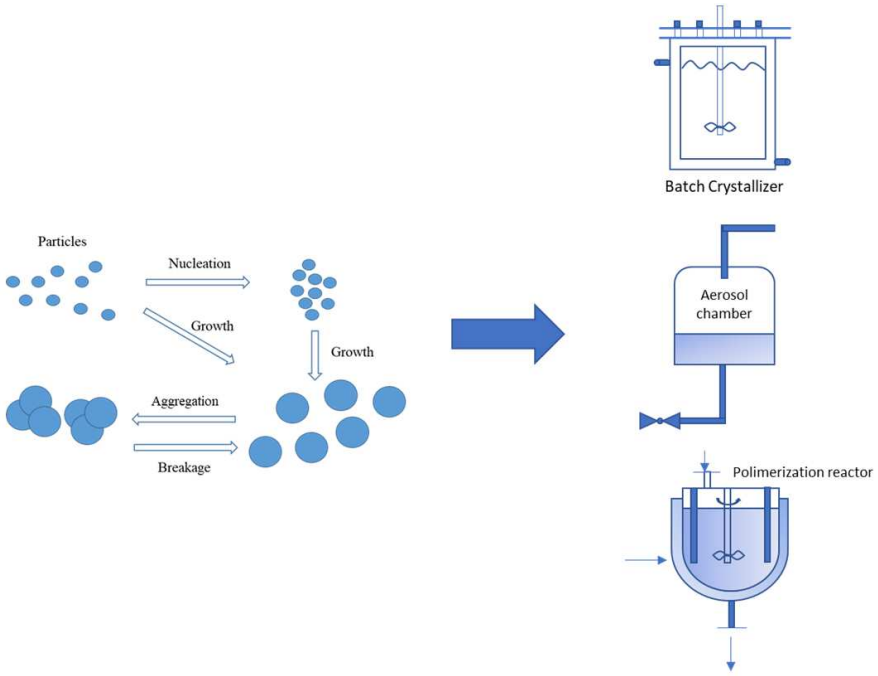

Fig. 1. Phenomena that govern the distribution of particles (Adapted from [18]).

2. Mathematical Models

The particle size distribution is determined by the influence of several physical-chemical phenomena, which are: nucleation, growth, aggregation, and breakage [1]. An illustration of this phenomenon is shown in Fig. 1.

The models that simulate the dynamics of these systems are called population balance [19-21]. The model that considers the main phenomena that influence the particle distribution dynamics is presented in eq. (1).

$$\frac{\partial n(v,t)}{\partial t} = \underbrace{-\frac{\partial\left[I_v(v,t)n(v,t)\right]}{\partial v}}_{(I)} + \underbrace{\frac{1}{2}\int_0^{v/2}\beta_v(v-\bar{v},\bar{v},t)n(v-\bar{v},t)n(\bar{v},t)d\bar{v}}_{(II)} - \underbrace{\int_0^{\infty}\beta_v(v,\bar{v},t)n(v,t)n(\bar{v},t)d\bar{v}}_{(III)} + \underbrace{S_v\left[n(v,t),v,t\right]}_{(IV)} \tag{1}$$

where $I_v(v,t)$ is the rate of change in volume v by mass transfer between particles and fluid phase, $\beta_v(v,\bar{v},t)$ is the particle coagulation coefficient for volumes v and $\bar{v}$, and S_v is the net rate of addition or removal of particles in the system.

Each term in eq. (1) represents a phenomenon: the parcel (I) is related to the rate of growth of particles by mass transfer to a single particle; the term (II) represents the generation of particles by the collision of a particle of size $v-\bar{v}$ with another of size $\bar{v}$ to form one of volume v (assuming the conservation of volume during coagulation); the term (III) represents the rate of particle death from the collision with other particles; the quantity (IV) represents the rate of addition or removal of particles in the system [20-21].

Due to the great variety of possibilities in which eq. (1) is inserted, Gelbard and Seinfeld [21] proposed four models, which are particular cases of the model represented by eq. (1), which will be detailed in the following topics.

2.1. Model 1: pure aggregation model with constant aggregation coefficient

Model 1 considers a particulate system submitted only to pure aggregation with a constant aggregation coefficient, which does not depend on the particles' size, i.e., $\beta_v(v,\bar{v},t)=\beta_0(t)$ [23]. In this model, the step of random coalescence controls the process of enlarging the particles. Therefore, it means that the particles' size is not considered when forming a stable agglomerate and that the coefficient is independent of the size. Thus, the population balance model in eq. (1) takes the form [20-22, 24]:

$$\frac{\partial n(v,t)}{\partial t} = \frac{\beta_0}{2}\int_0^{v} n(v-\bar{v},t)n(\bar{v},t)d\bar{v} - \beta_0\int_0^{\infty} n(v,t)n(\bar{v},t)d\bar{v} \tag{2}$$

where $\beta_0(t)$ is the constant aggregation coefficient.

Scott [24] presented an analytical solution for eq. (2), using the Laplace transform, resulting in the following expression:

$$n(v,t) = \frac{4\left(\frac{N_0}{v_0}\right)}{\left(2+\beta_0 N_0 t\right)^2}\exp\left[-\frac{2}{\left(2+\beta_0 N_0 t\right)}\frac{v}{v_0}\right] \tag{3}$$

In terms of the particle diameter, eq. (3) becomes:

$$n(D,t)=\frac{4\left(\frac{N_0}{v_0}\right)\left(\frac{D}{D_0}\right)^2}{\left(2+\beta_0 N_0 t\right)^2}\exp\left[-\frac{2}{\left(2+\beta_0 N_0 t\right)}\left(\frac{D}{D_0}\right)^3\right] \tag{4}$$

2.2. Model 2: pure aggregation model with linear aggregation coefficient

Model 2 considers that, during the aggregation process, the colliding particles' size is considered in the formation of an agglomerate. Also, larger particles have more favorable agglomeration than smaller ones [25]. The aggregation coefficient takes the form $\beta_v(v,\bar{v},t)=\beta_1(v+\bar{v})$, which is related to the turbulent diffusion [26,27]. From these considerations, eq. (1) takes the following form [20-22,24,26]:

$$\frac{\partial n(v,t)}{\partial t}=\frac{\beta_1}{2}\int_0^v (v+\bar{v})n(v-\bar{v},t)n(\bar{v},t)d\bar{v}-\beta_1 n(v,t)\int_0^\infty (v+\bar{v})n(\bar{v},t)d\bar{v} \tag{5}$$

where β_1 is the linear aggregation coefficient.

The mathematical model obtained by the partial integral-differential expression, eq. (5), admits an analytical solution. Scott [24] and Golovin [26] developed the analytical solution as follows:

$$n(v,t)=-\frac{N_0(1-T)}{v\sqrt{T}}\exp\left[-\frac{(1+T)v}{v_0}\right]I_1\left[2\sqrt{T}\,\frac{v}{v_0}\right] \tag{6}$$

where $T=1-\exp(-\tau)$, $\tau=\beta_1 N_0 v_0 t$, and I_1 is the modified Bessel function of first order. In terms of the particle diameter, eq. (6) becomes:

$$n(D,t)=-\frac{3(1-T)N_0}{D\sqrt{T}}\exp\left[-\frac{(1+T)D^3}{{D_0}^3}\right]I_1\left[2\sqrt{T}\left(\frac{D}{D_0}\right)^3\right] \tag{7}$$

2.3. Model 3: pure aggregation model with linear aggregation coefficient and particle removal rate

Model 3 considers a particulate system submitted to pure aggregation, whose linear aggregation coefficient is equal to $\beta_1(v+\bar{v})$, and R_0 represents the particle removal rate. The loss of particles to the container's inner surfaces can also be an important factor in changing the forms of particle size distribution. The main mechanisms for removing particles due to deposition are sedimentation and diffusion [28]. The population balance model for this case is presented as [21,22]:

$$\frac{\partial n(v,t)}{\partial t}=\frac{\beta_1}{2}\int_0^v (v+\bar{v})n(v-\bar{v},t)n(\bar{v},t)d\bar{v}-\beta_1 n(v,t)\int_0^\infty (v+\bar{v})n(\bar{v},t)d\bar{v}\text{-}R_0 n(v,t) \tag{8}$$

where β_1 is the linear aggregation coefficient and R_0 is the particle removal rate. Equation (8) admits an analytical solution in the form [21,22]:

$$n(v,t)=-\frac{\tilde{T}N_0}{v\sqrt{\tilde{g}}}\exp\left(\frac{\left(\tilde{T}-1\right)}{\theta}\right)\exp\left[-\left(1+\tilde{g}\right)\frac{v}{v_0}\right]I_1\left[2\sqrt{\tilde{g}}\,\frac{v}{v_0}\right] \tag{9}$$

where $\tilde{T}=\exp(-\Theta\tau)$, $\tau=\beta_1 N_0 v_0 t$, $\tilde{g}=1-exp\left((\tilde{T}-1)/\Theta\right)$, $\Theta=R_0/\beta_1 N_0 v_0$ and I_1 is the modified Bessel function of first order. In terms of the particle diameter:

$$n(D,t)=-\frac{3\tilde{T}}{D\sqrt{\tilde{g}}}\exp\left(\frac{\left(\tilde{T}-1\right)}{\theta}\right)\exp\left[-\left(1+\tilde{g}\right)\left(\frac{D}{D_0}\right)^3\right]I_1\left[2\sqrt{\tilde{g}}\left(\frac{D}{D_0}\right)^3\right] \tag{10}$$

2.4. Model 4: pure aggregation model with constant aggregation coefficient and linear growth rate

Model 4 considers a particulate system submitted to pure aggregation, whose aggregation coefficient is constant, and the particle growth rate by condensation is heterogeneous. Thus, the growth term in eq. (1) takes the form $I_v(v,t)=\sigma v$. Therefore, the population balance model is represented mathematically as [20,22,27]:

$$\frac{\partial n(v,t)}{\partial t}=-\sigma\frac{\partial\left[vn(v,t)\right]}{\partial v}+\frac{\beta_0}{2}\int_0^{v/2} n(v-\bar{v},t)n(\bar{v},t)d\bar{v}-\beta_0 n(v,t)\int_0^\infty n(\bar{v},t)d\bar{v} \tag{11}$$

where σ represents the difference in the concentration of diffusing species in the environment and on the particle surface, considering a growth rate controlled by the medium's chemical reaction. The analytical solution for eq. (11) is given by [20-22]:

$$n(v,t)=\frac{4\left(N_0/v_0\right)}{(2+\tau)^2}\exp\left[-\frac{2v}{(2+\tau)v_0}\exp(-\Lambda\tau)-\Lambda\tau\right] \tag{12}$$

where $\tau = \beta_0 N_0 v_0 t$ and

$$\Lambda = \frac{\sigma}{\beta_0 N_0} \tag{13}$$

In terms of the particle diameter:

$$n(D,t) = \frac{4\left(N_0/D_0\right)\left(D/D_0\right)^2}{(2+\tau)^2}\exp\left[-\frac{2D^3}{(2+\tau)D_0{}^3}\exp(-\Lambda\tau) - \Lambda\tau\right] \tag{14}$$

Although there are other models present in the literature to describe the population dynamics of particles in the environment, we consider the models proposed by Gelbard and Seinfeld [21] because they present analytical solutions that are easy to implement and have low computational cost.

3. Inverse Problem

Bayes' theorem allows combining the information obtained by the experiments with that obtained from a mathematical model. Considering a vector of parameters, $\boldsymbol{\theta}^T = [\theta_1, \theta_2, \theta_3, ..., \theta_p]$, and a vector of measurements, $\mathbf{Y}^T = [Y_1, Y_2, Y_3, ..., Y_m]$, where p and m represent the numbers of parameters and measures, respectively. Bayes' theorem can be written as [29-40]:

$$\pi(\boldsymbol{\theta}|\mathbf{Y}) = \frac{\pi_{priori}(\boldsymbol{\theta})\pi(\mathbf{Y}|\boldsymbol{\theta})}{\pi(\mathbf{Y})} \tag{15}$$

where $\pi(\boldsymbol{\theta}|\mathbf{Y})$ is the *a posteriori* probability density, that is, the conditional density of the parameters $\boldsymbol{\theta}$ given the measures $\mathbf{Y}$; $\pi_{priori}(\boldsymbol{\theta})$ is the *a priori* probability density of the parameters, that is, the information encoded for the parameters available before the experimental measurements; $\pi(\mathbf{Y}|\boldsymbol{\theta})$ is the likelihood function that expresses the evidence of the measures $\mathbf{Y}$ given the parameters $\boldsymbol{\theta}$; and $\pi(\mathbf{Y})$ is the marginal probability density of the measures, which plays the role of a normalization constant. Bayes' theorem can also be written as [29-40]:

$$\pi(\boldsymbol{\theta}|\mathbf{Y}) \propto \pi_{priori}(\boldsymbol{\theta})\pi(\mathbf{Y}|\boldsymbol{\theta}) \tag{16}$$

3.1 Sensitivity analysis

One way to evaluate the sensitivity of the mathematical model parameters' estimates is by analyzing the sensitivity coefficient, J_{ij}, whose measure represents the sensitivity of a state variable, Y_i, concerning the variations of a given parameter, θ_i. In addition to providing information on the magnitude of the estimated parameters' sensitivity, this analysis allows the assessment of the linear dependence between the parameters. Suppose the magnitude of J_{ij} shows small values. In that case, this indicates that large variations in θ_i will result in small changes in Y_i, making the estimation of this parameter extremely difficult since the same amount of Y_i can be obtained for a wide range of values of θ_i. In addition to analyzing the magnitude of the sensitivity coefficient, the estimated parameters need to be linearly independent. The relationship between variations in parameters concerning the state variable can be represented by [29,32,36,37]:

$$J_{ij} = \frac{\partial Y_j}{\partial \theta_i} \tag{17}$$

Many engineering problems involve parameters with different orders of magnitude, making it difficult to compare and identify the linear dependence between the coefficients since these will present other orders of magnitude. One way to facilitate the comparison of the importance of the coefficients with the observable variables and the linear dependence analysis is to multiply them by the parameters to which they relate, obtaining the reduced sensitivity coefficient. This way, they will have the same units as the observable variables, thus providing a basis for comparisons. Then, the reduced sensitivity coefficient is defined as [32,36,37]:

$$X_{ij} = \theta_i \frac{\partial Y_j}{\partial \theta_i} \tag{18}$$

3.2 Markov chain Monte Carlo approach

In many cases within the Bayesian structure, it is impossible to obtain an analytical solution for the posterior probability distribution. In such cases, simulation methods, which use a sampling process to get information about the probability density a posteriori, can be used, as is the case with the Markov chain Monte Carlo (MCMC) approach [29,30,33-38].

The MCMC combines the properties of Monte Carlo and the Markov chain. The first is estimating the properties of distribution by examining random samples from the distribution. On the other hand, the second is based on the idea that a given sequential process generates random samples, where each random selection is used as a step to develop the next one. A particular property is that, although each new choice depends on the previous one, new samples do not rely on any instance before the last one [41].

One of the most widely used algorithms for implementing the Markov chain Monte Carlo is the Metropolis-Hastings. This algorithm uses a proposal distribution, $q(\boldsymbol{\theta}^*|\boldsymbol{\theta}^{(i)})$, to generate a vector of candidate parameters, $\boldsymbol{\theta}^*$, based on the chain's current state, $\boldsymbol{\theta}^{(i)}$. The Markov chain then moves to $\boldsymbol{\theta}^*$ with the probability of acceptance as given [29,30,33-38]:

$$\alpha\left(\boldsymbol{\theta}^{(i)},\boldsymbol{\theta}^{*}\right)=\min\left[1,\frac{p\left(\boldsymbol{\theta}^{*}\middle|\mathbf{Y}\right)q\left(\boldsymbol{\theta}^{(i)}\middle|\boldsymbol{\theta}^{*}\right)}{p\left(\boldsymbol{\theta}^{(i)}\middle|\mathbf{Y}\right)q\left(\boldsymbol{\theta}^{*}\middle|\boldsymbol{\theta}^{(i)}\right)}\right] \tag{19}$$

The Metropolis-Hastings algorithm can be specified by the following steps [29,30,33-35,38,39-43]:

1. Start the iteration counter, i = 1, and specify an initial value, $\boldsymbol{\theta}^{1}$;
2. Generate a vector of candidate parameters from the proposal distribution. In the present work, the proposed distribution used was Gaussian, according to:

$$\boldsymbol{\theta}^{*}=\boldsymbol{\theta}^{(i)}\left(1+\mathbf{w}\xi\right) \tag{20}$$

where ξ is a random variable N(0,1) and $\mathbf{w}$ is the search step;

1. Calculate the probability of acceptance, $\alpha\left(\boldsymbol{\theta}^{(i)},\boldsymbol{\theta}^{*}\right)$, given by eq. (19);
2. Generate an auxiliary random sample from the uniform distribution, $u \sim U(0,1)$;
3. If $u \le \alpha$, then accept the new value and update the parameter vector, $\boldsymbol{\theta}^{(i+1)}=\boldsymbol{\theta}^{*}$. Otherwise, $\boldsymbol{\theta}^{(i+1)}=\boldsymbol{\theta}^{(i)}$;
4. Increment the counter of i to i + 1 and go back to step 2.

4. Results and Discussion

The MCMC method with the accept/rejection Metropolis-Hastings algorithm was applied to estimate the parameters of the models proposed by Gelbard and Seinfeld [21]. By using simulated measures, it was possible to verify the algorithm implemented. The particle size distribution, $n(D,t)$, was used to generate measurements, where Gaussian noises were added, with zero mean and constant standard deviation. The simulated measurements were obtained according to:

$$n_{meas}=n_{exact}+\sigma_{meas}\xi \tag{21}$$

where n_{exact} is the solution of the forward problem with known parameters, σ_{meas} is the standard deviation of the measurements, and ξ is a random variable from distribution N(0,1).

We made estimates considering the Gaussian probability as prior distributions in the selected models. For the simulations, we chose the initial number of particles $N_0 = 1$ cm^{-3}, and the initial particle diameter $D_0 = 1$ μm. The analyzed times were 0, 0.4, 0.8, 1.2, 1.6, and 2 seconds. The simulations for the particle distribution, n, considering the four models in the present analysis, were based on the following hypotheses:

- Model 1: pure aggregation with constant aggregation coefficient, composed of one parameter $\boldsymbol{\theta}^{T}=[\beta_0]$ representing this coefficient;
- Model 2: pure aggregation with the linear aggregation coefficient, composed of one parameter $\boldsymbol{\theta}^{T}=[\beta_1]$ representing this coefficient;
- Model 3: pure aggregation with linear aggregation coefficient and particle removal rate, composed of two parameters $\boldsymbol{\theta}^{T}=[\beta_1,\mathrm{R}_0]$ representing these coefficients;
- Model 4: pure aggregation model with constant aggregation coefficient and linear growth rate, composed of two parameters $\boldsymbol{\theta}^{T}=[\beta_0,\sigma]$ representing the constant aggregation coefficient and the particle growth rate, respectively.

4.1 Analysis of model parameters

Before the sensitivity analysis, a parameter analysis was performed for the models with two parameters: models 3 and 4. These models are similar to models 2 and 1, respectively, since they have standard parameters, β_1 (linear aggregation coefficient), and β_0 (constant aggregation coefficient). However, models 3 and 4 also have additional parameters, which are the particle removal rate, R_0, and the particle growth rate, σ, respectively.

First, a numerical analysis was performed on models 3 and 4 to estimate the parameters R_0 (model 3), using the measurements generated by model 2, and σ (model 4), using the measurements generated by model 1. For this purpose, these parameters must have values that approximate the models to each other.

Because of the similarities between models 1 and 4 and models 2 and 3, numerical experiments were carried out to verify the solutions. Different values were assigned to the parameters that differentiate similar models from each other. When performing the analysis for models 3 and 4, numerical experiments were performed to determine which values of R_0 and σ approximate models 3 and 4 to models 2 and 1, respectively. Three values for particle removal rate were analyzed: 1, 0.30, and 0.01 cm³/s. For linear agglomeration rate, β_1 , it has been established $\beta_1 = 1$ cm³/s. For the growth rate, three values were also analyzed: 1, 0.10, and 0.01 cm³/s. For the constant agglomeration rate, β_0 , the value of $\beta_0 = 1$ cm³/s was admitted. The results of these analyses are shown in Figure 2.

Figure 2a shows that for the three R_0 values evaluated, the value that approximates model 3 to model 2 is 0.01 cm³/s, which is the lowest of the established values. This result is related to the small influence that the removal rate has on the particle size distribution density, the dynamics of this medium being controlled by the linear aggregation rate, as in model 2, where agglomeration is the only physical phenomenon involved. Figure 2b shows that the value of σ , which approximates model 4 to model 1, is $\sigma = 0.01$ cm³/s because the lower the amount of σ , the greater is the influence of aggregation on the particle size distribution density. In this way, the process is controlled only by the collision between particles to form stable aggregates, as in model 1.

With the results obtained in Fig. 2, the next step was the sensitivity analysis for the parameters of models 3 and 4, followed by estimates by the Markov Chain Monte Carlo method. For these inferences, based on the analysis of model parameters, we have used the reference parameters contained in Table 1.

4.2 Sensitivity analysis

The sensitivity analyses were performed through the reduced sensitivity coefficients applied to models 3 and 4. The parameter values were chosen based on the numerical analysis, according to Table 1.

Table 1. Reference parameters for the models proposed by Gelbard and Seinfeld [21].

Parameter	Model	Value (unit)
β_0	1 and 4	1 cm³/s
β_1	2 and 3	1 cm³/s
R_0	3	0.01 cm³/s
σ	4	0.01 cm³/s

Model 3 consists of two parameters, the linear aggregation coefficient, β_1, and the particle removal rate, R_0. Sensitivity coefficients are presented for different particle diameter measurements, i.e., D = [1, 1.5, 2, 2.5], in micrometers, to verify the linear dependence and the magnitude. These coefficients are shown in Figure 3 for each of the diameters analyzed.

Figure 3 indicates that the reduced sensitivity coefficients related to the model 3 parameters are linearly independent in all cases analyzed. The parameter β_1 presented a considerable magnitude to the size distribution density function for all diameters. Regarding the parameter R_0, a low magnitude was obtained in all diameters analyzed. This fact is related to the reference value used for the removal rate, which approximates model 3 to model 2, making low the parameter's sensitivity.

A similar analysis was done for the parameters of model 4 (aggregation coefficient, β_0, and growth rate, σ). Such analysis is shown in Fig. 4, and it indicates that the reduced sensitivity coefficients related to this model parameters are also linearly independent in all cases analyzed.

4.3 Estimation parameter of model 3 using the MCMC approach

Estimation of model 3 parameters β_1 and R_0 were performed using the MCMC method. Candidate parameters were generated using a Gaussian transition kernel, whose mean is equal to the previous state parameter. The standard deviation is the search step, **w**, multiplied by the last state parameter. Some measurements generated from model 2 were used to estimate the model 3 parameters since both have the same parameter, β_1.

A Gaussian probability distribution was considered *a priori* for the model 3 estimations. Means were fixed in the parameter reference values and standard deviations of 10 and 0.4% to the parameters β_1 and R_0, respectively. The measurement uncertainty was 1%, with the maximum value of the state variable. The analyzed case is shown in Table 2, where n_{exact} represents the forward solution of model 2 for generating measurements.

For the application of the Markov chain Monte Carlo method, 10^4 states and search step equal to 0.004 were used. The initial estimations of each parameter were considered twice the reference value of β_1, whereas we used the reference value for R_0. These estimates were established from the sensitivity coefficient analysis, whose results showed low sensitivity for the parameter R_0. Figure 5 shows the evolution of the Markov chains of the parameters β_1 and R_0. For both parameters, approximately 1000 burn-in states were required until the convergence of Markov chains.

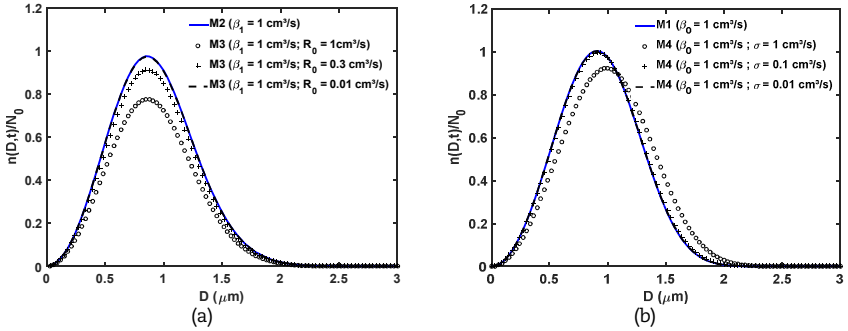

Fig. 2. Dynamics numerical analysis for: (a) parameters of model 3; (b) parameters of model 4.

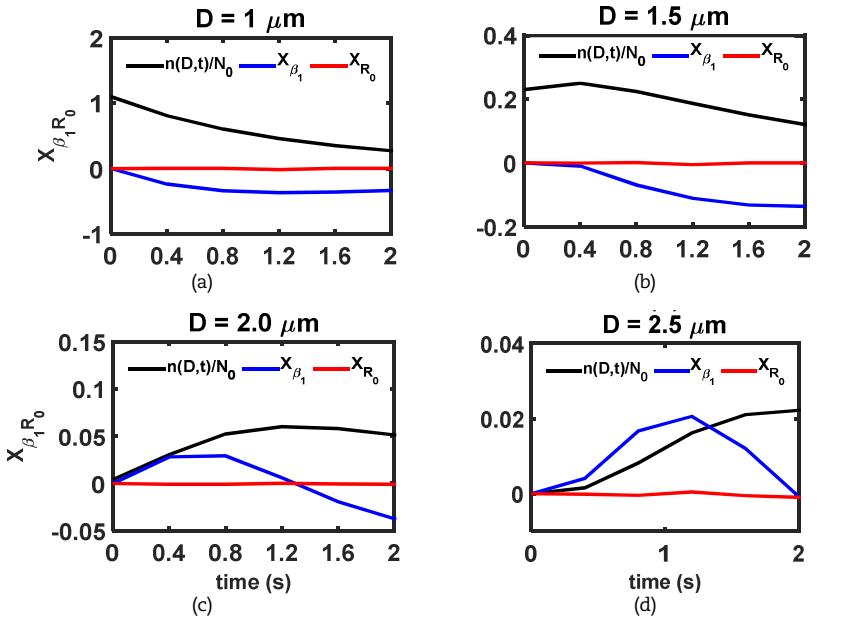

Fig. 3. Analysis of reduced sensitivity coefficients for the parameters of the model 3.

Table 2. Values for the estimation of model 3 parameters.

σ_{meas}	Prior distribution (Gaussian)			
	μ_{R_0}	μ_{β_1}	σ_{β_1}	σ_{R_0}
$1\% \max(n_{exact})$	R_0^{Ref}	β_1^{Ref}	$0.1\beta_1^{Ref}$	$0.004R_0^{Ref}$

Figure 6 shows the autocorrelations for the parameters β_1 and R_0. Autocorrelation measures the correlation between points in the chain separated by several lags of Markov states, informing how the chain's current conditions are correlated with the previous ones. For the generation of this autocorrelation, we discarded the samples obtained during the chain's burn-in period (1000 states) since the distribution of these samples differs significantly from the initial one in this period. It was found that the autocorrelation for β_1 parameter rapidly decreased to zero, and, upon reaching approximately 20 lags, the stationary chain samples were no longer correlated.

Regarding the R_0 parameter's autocorrelation, it was observed that it took a long time for the samples to become non-correlated, approximately 40 lags. This analysis is essential since the correlated chains can cause errors. Therefore, the estimates were performed using points in the chain with an interval of 40 lags between them.

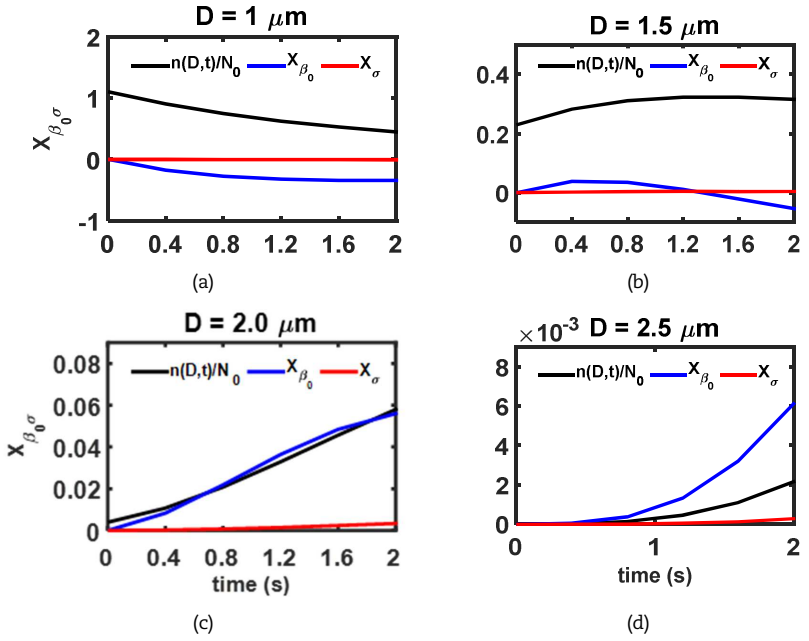

Fig. 4. Analysis of reduced sensitivity coefficients for the parameters of the model 4.

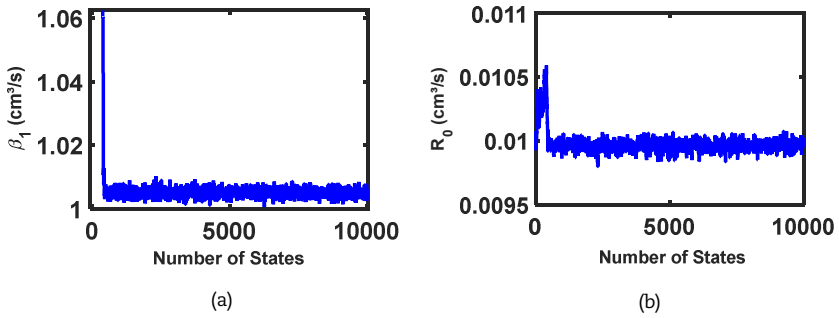

Fig. 5. Evolution of the Markov chain for the parameters β_1 and R_0.

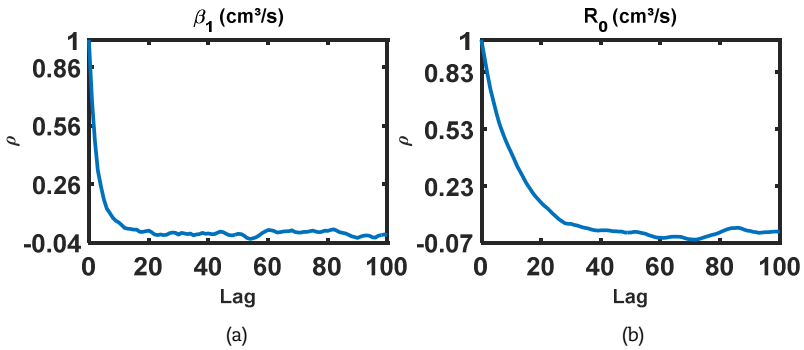

Fig. 6. Autocorrelation of model 3 parameters.

Figure 7 shows the comparisons between the estimated, exact, and measured size distribution density function of model 3. Measures over time using a reference diameter for the particle of 1 μm were considered (Figure 7.a), with measurements in all particle diameters, evaluated at times of 0.8; 1.2; 1.6; and 2 seconds (Figure 7.b). The density function was obtained using the estimated parameters after verifying the autocorrelation of the chain. Figure 7 indicates that the calculated and measured density showed good agreement in the analyzed profiles since they are within or close to the established credibility interval, which was 99%. The results showed that the size distribution density function decreases when the time increases and, consequently, the diameter also increases. This fact is due to the collision between particles to form larger bodies.

Figure 8 shows the residual (the difference between the estimated and exact solution) and the relative error between the measurements generated from model 2 and the estimates obtained for model 3. It appears that the residues had a low magnitude, on the order of 1000 times lower than the state variable, indicating a satisfactory adjustment of the estimated density function for model 3 in comparison with the simulated measurements of model 2. A value of 2% was obtained regarding the relative error, confirming the excellent fit between the estimated densities and the measurements.

Simulation acceptance rates for estimating parameters and RMS errors that quantify the discrepancy between predicted and simulated measures were also calculated. For the acceptance rate considering 10,000 states, the value found was 0.16, and an RMS error of 0.0776.

The mean and the credibility interval of the posterior probability distributions of the estimated parameters were also evaluated, whose results are shown in Table 3. It appears that the estimates were accurate since the parameters are within the 99% credibility range and accuracy, as they are close to the reference values.

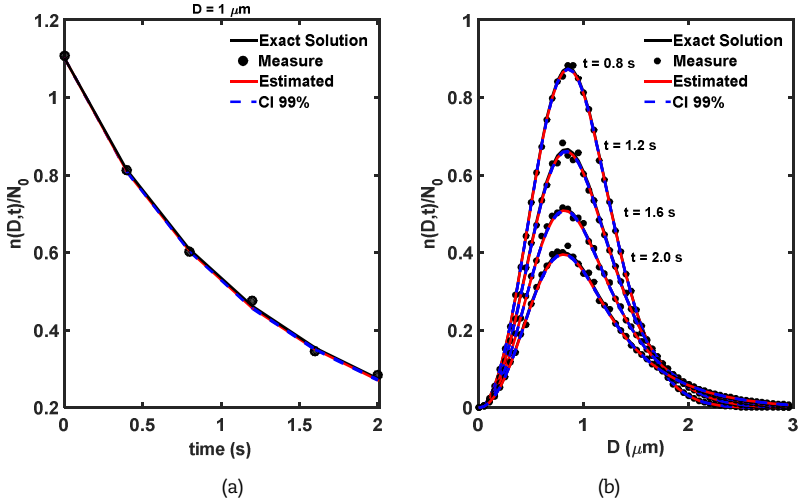

Fig. 7. Comparison among the estimated, exact and measured density function of model 3.

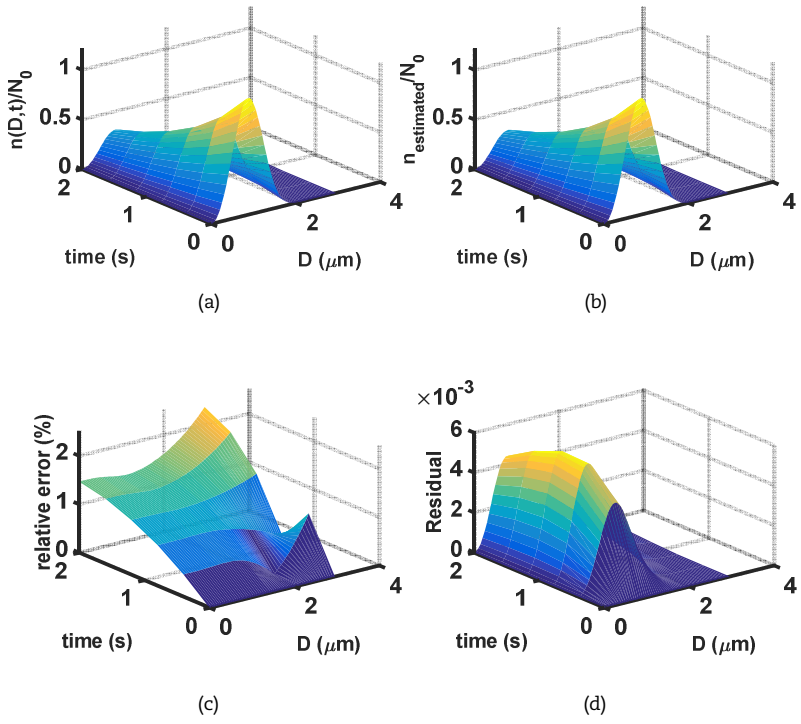

Fig. 8. Analysis of residuals and relative errors when using measures generated by model 2.

Table 3. Estimation of parameters (mean and 99% credibility interval).

	Prior distribution (Gaussian)				Estimated	
σ_{meas}	μ_{R_0}	μ_{β_1}	σ_{β_1}	σ_{R_0}	β_1	R_0
$1\% \max(n_{exact})$	R_0^{Ref}	β_1^{Ref}	$0.1\beta_1^{Ref}$	$0.004R_0^{Ref}$	1.005 (1.002; 1.009)	0.01 (0.009; 0.01)

Table 4. Values for the estimation of model 4 parameters.

	Prior distribution (Gaussian)			
σ_{meas}	μ_{β_0}	μ_{σ}	σ_{β_0}	σ_{σ}
$5\% \max(n_{exact})$	β_0^{Ref}	σ^{Ref}	$0.1\beta_0^{Ref}$	$0.004\sigma^{Ref}$

4.4 Estimation parameter of model 4 using the MCMC approach

The estimations of model 4 parameters β_0 and σ were performed using the Markov chain Monte Carlo method. For this purpose, measures generated from model 1 were utilized due to the presence of parameter β_0 in both models. Also, for the model 4 estimations, a priori Gaussian probability distribution was considered, with the mean-centered on the reference values of the parameters and standard deviations of 10 and 0.4% of the reference value for β_0 and σ , respectively. The measurement uncertainty was 5% to the maximum amount of the state variable. The analyzed case is presented in Table 4, where n_{exact} represents the forward solution of model 1.

Figure 9 shows the evolution of the Markov chains for parameters β_0 and σ . In this case, an uncertainty of 5% was established to the maximum value of the size distribution density function. Results showed that the chains for β_0 and σ converged to values close to the reference after approximately 500 states of the Markov chain (burn-in states).

After defined the burn-in states, we carried out the correlation analysis of the parameters, as shown in Figure 10. The autocorrelation for parameter β_0 reached quickly the value zero, while for parameter σ , this convergence was slower, indicating that, in this case, the chain states are more correlated. From 40 lags, the chain states of the two parameters showed zero correlation. Therefore, to obtain the estimations, we used points with intervals of 40 lags between them.

Figure 11 shows the comparisons between the estimated, exact, and measured size distribution density function of model 4, whose results showed a good agreement with each other. The analysis indicated that the size distribution density function decreases when time increases. Consequently, the diameter also increases because it is related to the collision between particles to form larger particles.

Figure 12 shows the residual and the relative error between the measurements generated from model 1 and the estimations of model 4. The residues presented a low magnitude, with values in the order of 100 times less than the state variable, indicating that the estimated density function showed a reasonable adjustment when compared with the simulated measures. Similarly, it was observed for the relative error, with a value in the order of 5%, confirming the excellent fit between the estimated densities and the measurements.

Simulation acceptance rates for estimating parameters and RMS errors that quantify the discrepancy between predicted and simulated measures were also calculated. For the acceptance rate considering 10,000 states, the value found was 0.50 and the RMS error 0.0043.

Table 5 presents the results in terms of the mean and the 99% credibility interval of the *a posteriori* probability distributions of the parameters β_0 and σ , whose values showed good precision and accuracy.

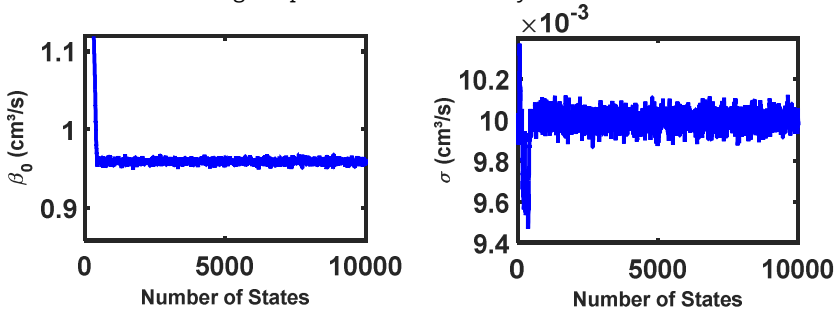

Fig. 9. Evolution of the Markosv chain for the parameters β_0 and σ.

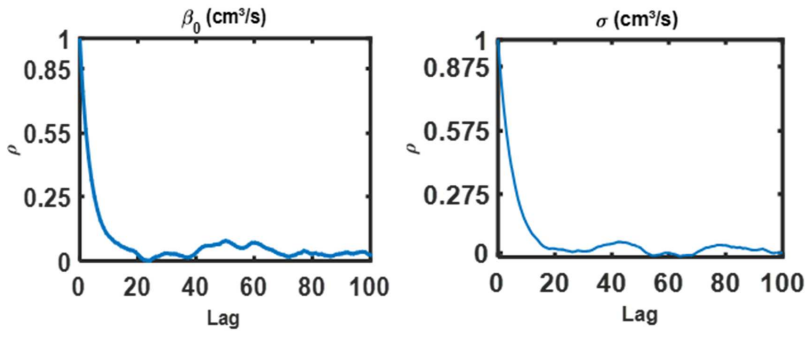

Fig. 10. Autocorrelation of model 4 parameters.

Table 5. Estimation of parameters (mean and 99% credibility interval).

	Prior distribution (Gaussian)				Estimated	
σ_{meas}	μ_{β_0}	μ_{σ}	σ_{β_0}	σ_{σ}	β_0	σ
5% $\max(n_{exact})$	β_0^{Ref}	σ^{Ref}	$0.1\beta_0^{Ref}$	$0.004\sigma^{Ref}$	0.959 (0.951; 0.965)	0.01 (0.0099; 0.0101)

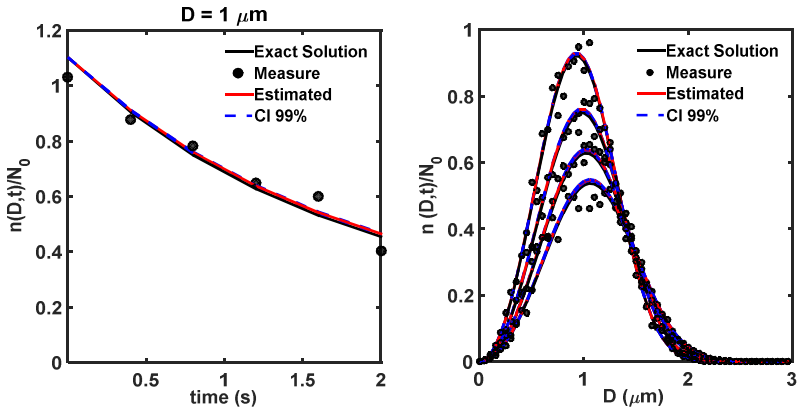

(a) (b)

Fig. 11. Comparison among the estimated, exact and measured density function of model 4.

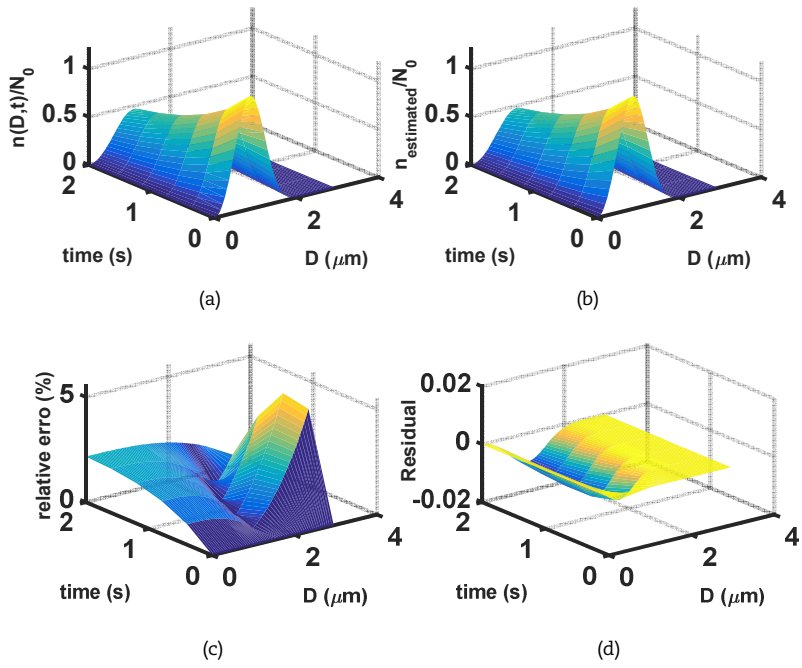

(a) (b) (c) (d)

Fig. 12. Analysis of residuals and relative errors when using measures generated by model 1.

5. Conclusions

In this work, we used the Bayesian Markov chain Monte Carlo technique to estimate the parameters of the four models proposed by Gelbard and Seinfeld [21], which have the particle size distribution density function $n(D,t)$ as the only state variable. The reduced sensitivity coefficients analysis showed a considerable magnitude concerning the parameters β_1 and R_0 (model 3) and β_0 and σ (model 4). It was possible to estimate the parameters of models 3 and 4, respectively, using simulated measurements obtained from models 2 and 1 in different scenarios, considering a priori Gaussian probability distribution for the parameters. The Markov chains of the estimated parameters, in all evaluated cases, converged to values close to the reference. The autocorrelation analysis between the chain states allowed us to obtain reliable estimations since we not considered points in the chain correlated with each other. In all the scenarios evaluated, the parameter estimates showed precision and accuracy. Besides, we found a good agreement between the estimated state variables and the measures, with residues in the order of 1000 and 100 times for the cases analyzed for models 3 and 4, respectively, indicating that the Markov chain Monte Carlo method can be used to estimate rates that influence population dynamics in these models.

Author Contributions

Carlos H.R. Moura and Bruno M. Viegas analyzed the physical meaning of models used to describe the population balance; João N.N. Quaresma and Emanuel N. Mâcedo developed the mathematical modeling; Carlos H.R. Moura, Diego C. Estumano and

Maria R.M. Tavares applied the Markov Chain Monte Carlo in the models. The manuscript was written through the contribution of all authors. All authors discussed the results, reviewed, and approved the final version of the manuscript.

Acknowledgments

The authors thank the CNPq, CAPES, FINEP and PROPESP/UFPA for their financial support.

Conflict of Interest

The authors declared no potential conflicts of interest with respect to the research, authorship, and publication of this article.

Funding

This work was supported by the CNPq, CAPES, FINEP and PROPESP/UFPA.

Nomenclature

D	Particle diameter [μm]	α	Probability of acceptance in the Metropolis-Hastings algorithm
D_0	Initial particle diameter [μm]	β_0	Constant coagulation coefficient [cm³.s⁻¹]
$I_v(v,t)$	Volume change rate of a particle of volume v by mass transfer between particles and fluid phase [cm³.s⁻¹]	β_1	Linear coagulation coefficient [cm³.s⁻¹]
J_{ij}	Sensitivity coefficient	μ	Mean
$n(v,t)$	Size distribution density function [μm⁻³.cm⁻³]	θ	Parameter vector
$n(D,t)$	Size distribution density function as a function of diameter [μm⁻¹.cm⁻¹]	ρ	Correlation coefficient
N_0	Total number of particles at time zero [cm⁻³]	σ	Growth rate [cm³.s⁻¹]
$q(\theta \mid \theta^*)$	Proposal distribution	σ_{meas}	Measure deviation
R_0	Removal rate[cm³.s⁻¹]	σ_p	Standard deviation
S_v	Rate of addition or removal of particles in the system [cm³.s⁻¹]	τ	Dimensional time
X_{ij}	Reduced sensitivity coefficient	ξ	Random variable with normal distribution and zero mean
w	Search step		
Y	Measures vector		

References

[1] Randolph, A.D., Larson, M.A., *Theory of Particulate Processes*, second ed. Academic Press, San Diego, CA, 1988.
[2] Henson, M.A., Dynamic modeling of microbial cell populations, *Current Opinion in Biotechnology*, 14, 2003, 460-467.
[3] Vale, H.M., Mckenna, T.F., Modeling particle size distribution in emulsion polymerization reactors, *Progress in Polymer Science*, 30, 2005, 1019-1048.
[4] Alexopoulos, A.H., Roussos, A.I., Kiparissides, C., Part I: Dynamic evolution of the particle size distribution in particulate processes undergoing combined particle growth and aggregation, *Chemical Engineering Science*, 59, 2004, 5751-5769.
[5] Roussos, A.I., Alexopoulos, A.H., Kiparissides, C., Part III: Dynamic evolution of the particle size distribution in batch and continuous particulate processes: A Galerkin on finite elements approach, *Chemical Engineering Science*, 60, 2005, 6998-7010.
[6] Hulburt, H.M., Katz, S., Some problems in particle technology: A statistical mechanical formulation, *Chemical Engineering Science*, 19, 1964, 555-574.
[7] Ramkrishna, D., *Population Balances: Theory and Applications to Particulate Systems in Engineering*, first ed. Academic Press, San Diego, CA, 2000.
[8] Hede, P.D., *Modelling batch fluid bed granulation processes using population balances*, Bookboon, Copenhagen, DK, 2006.
[9] Groh, A., Parameter Estimation in Population Balance Model, *AIP Conference Proceedings*, American Institute of Physics, 2010.
[10] Ramachandran, R., Barton, P.I., Effective parameter estimation within a multi-dimensional population balance model framework, *Chemical Engineering Science*, 65, 2010, 4884-4893.
[11] Solsvik, J., Becker, P.J., Sheibat-Othman, N., Jakobsen, H.A., Population balance model: Breakage kernel parameter estimation to emulsification data, *Canadian Journal of Chemical Engineering*, 92, 2014, 1082-1099.
[12] Besenhard, M.O., Chaudhury, A., Vetter, T., Ramachandran, R., Khinast, J.G., Evaluation of Parameter Estimation Methods for Crystallization Processes Modeled via Population Balance Equations, *Chemical Engineering Research and Design*, 94, 2015, 275-289.
[13] Rosle, M. S., et al., A Hybrid of Particle Swarm Optimization and Harmony Search to Estimate Kinetic Parameters in Arabidopsis thaliana, *Processes*, 8(8), 2020, 921.
[14] Zhang, Z., Jun L.,Yaowu S., Application of artificial bee colony algorithm to maximum likelihood DOA estimation, *Journal of Bionic Engineering*, 10(1), 2013, 100-109.
[15] Pilania, G., et al., Prediction of structure and cation ordering in an ordered normal-inverse double spinel, *Communications Materials*, 1(1), 2020, 1-11.
[16] Lu, X. and Boleslaw K. S., A Regularized Stochastic Block Model for the robust community detection in complex networks, *Scientific Reports*, 9(1), 2019, 1-9.
[17] Yao, Z., et al., Compton-based prompt gamma imaging using ordered origin ensemble algorithm with resolution recovery in proton therapy, *Scientific Reports*, 9(1), 2019, 1-15.
[18] Ilievski, D., White, E.T., Agglomeration during precipitation: agglomeration mechanism identification for $Al(OH)_3$ crystals in stirred caustic aluminate solutions, *Chemical Engineering Science*, 49, 1994, 3227-3239.
[19] Drake, R.L., *Topics in Current Aerosol Research*, Pergamon, Oxford, UK, 1972.
[20] Ramabhadran, T.E., Peterson, T.W., Seinfeld, J.H., Dynamics of aerosol coagulation and condensation, *AIChE Journal*, 22, 1976, 840-851.
[21] Gelbard, F., Seinfeld, J.H., Numerical solution of the dynamic equation for particulate systems, *Journal of Computational Physics*, 28, 1978, 357-375.
[22] Peterson, T.W., Gelbard, F., Seinfeld, J.H., Dynamics of source-reinforced, coagulating, and condensing aerosols, *Journal of Colloid And Interface Science*, 63, 1978, 426-445.
[23] Kapur, P.C., Fuerstenau, D.W., A coalescence model for granulation, *Industrial and Engineering Chemistry Process Design and Development*, 8, 1969, 56-62.
[24] Scott, W.T., Analytical Studies of Cloud Droplet Coalsecnce, *Journal of the Atmospheric Sciences*, 25, 1968, 54-65.
[25] Salman, A.D., Hounslow, M.J., Seville, J.P.K., *Handbook of Powder Technology: Granulation*, Elsevier Science, Amsterdam, NH, 2007.
[26] Golovin, A. M., The Solution of the Coagulation Equation for Raindrops. Taking Condensation into Account, *Soviet Physics Doklady*, 8, 1963, 191-193.
[27] Hidy, G.M., Brock, J.R., *The Dynamics of Aerocolloidal Systems*, Pergamon, Oxford, UK, 1970.
[28] Slama, M., Shaker, M.O., Aly, R., Sirwah, M., Applications of aerosol model in the reactor containment, *Journal of Radiation Research and Applied Sciences*, 7, 2014, 499-505.
[29] Orlande, H.R.B., Inverse Problems in Heat Transfer: New Trends on Solution Methodologies and Applications, *ASME Journal of Heat Transfer*, 134(3),

2012.
[30] Abreu, L.A.S., H. R. B. Orlande, M. J. Colaço, J. Kaipio, V. Kolehmainen, and R.M. Cotta, Detection of Contact Failures with the Markov Chain Monte Carlo Method by Using Integral Transformed Measurements, *International Journal of Thermal Sciences*, 132, 2018, 486-497.
[31] Lamien, B., H.R.B. Orlande, L.A. Bermeo Váron, R.L.Q. Basto, G.E. Eliçabe, D.S. Santos, and R.M. Cotta, Estimation of the Temperature Field in Hyperthermia Experiments with a Phantom, *International Journal of Hyperthermia*, 35(1), 2018, 279-290.
[32] Silva, G.R., D.C. Knupp, C.P. Naveira-Cotta, R.M. Cotta, and A.J. Silva Neto, Estimation of Slip Flow Parameters in Microscale Conjugated Heat Transfer Problem, *Journal of the Brazilian Society of Mechanical Sciences and Engineering*, 42, 2020, 263.
[33] Kaipio, J., Somersalo, E., *Statistical and Computational Inverse Problems*, Springer, New York, NY, 2004.
[34] Pasqualette, M.A., Estumano, D.C., Hamilton, F.C., Colaço, M.J., Leiroz, A.J.K.; Orlande, H.R.B.; Carvalho, R.N.; Dulikravich, G.S., Bayesian estimate of pre-mixed and diffusive rate of heat release phases in marine diesel engines, *Journal of the Brazilian Society of Mechanical Sciences and Engineering*, 39, 2017, 1835-1844.
[35] Oliveira, R. F., Nunes, K. G. P., Jurado, I. V., Amador, I. C. B., Estumano, D. C., & Féris, L. A., Cr (VI) adsorption in batch and continuous scale: A mathematical and experimental approach for operational parameters prediction, *Environmental Technology & Innovation*, 20, 2020, 1092-1105.
[36] Beck, J.V., Blackwell, B., Clair, C.R.S., *Inverse Heat Conduction: III-Posed Problems*, Wiley-Interscience, New York, NY, 1985.
[37] Ozisik, M.N., Orlande, H.R.B., *Inverse Heat Transfer: Fundamentals and Applications*, Taylor & Francis, New York, 2000.
[38] Orlande, H.R.B., Colaço, M.J., Dulikravich, G.S., Approximation of the likelihood function in the Bayesian technique for the solution of inverse problems, *Inverse Problems in Science and Engineering*, 16, 2008, 677-692.
[39] Estumano, D.C., et al., Bayesian estimate of mass fraction of burned fuel in internal combustion engines using pressure measurements, *Engineering Optimization*, 5, 2015, 997-1003.
[40] Ma, Z., et al., Bayesian estimation of Dirichlet mixture model with variational inference, *Pattern Recognition*, 47(9), 2014, 3143-3157.
[41] Van Ravenzwaaij, D., Cassey, P., Brown, S.D., A simple introduction to Markov Chain Monte-Carlo sampling, *Psychonomic Bulletin & Review*, 25, 2018, 143-154.
[42] Metropolis, N., Rosenbluth, A.W., Rosenbluth, M.N., Teller, A.H., Teller, E., Equation of state calculations by fast computing machines, *Journal of Chemical Physics*, 21, 1953, 1087-1092.
[43] Hastings, W.K., Monte Carlo sampling methods using Markov Chains and their applications, *Biometrika*, 57, 1970, 97-109.

ORCID iD

Carlos H.R. Moura https://orcid.org/0000-0002-1407-3089
Bruno M. Viegas https://orcid.org/0000-0002-2768-652X
Maria R.M. Tavares https://orcid.org/0000-0001-6990-9122
Emanuel N. Macêdo https://orcid.org/0000-0002-4652-8316
Diego C. Estumano https://orcid.org/0000-0003-4318-4455
João N.N. Quaresma https://orcid.org/0000-0001-9365-7498

How to cite this article: Moura C.H.R., Viegas B.M., Tavares M.R.M., Macêdo E.N., Estumano D.C., Quaresma J.N.N. Parameter estimation in population balance through Bayesian technique Markov Chain Monte Carlo, *J. Appl. Comput. Mech.*, 7(2), 2021, 890–901. https://doi.org/10.22055/JACM.2021.35741.2725